Accepted Manuscript

Effect of UV irradiation and physical aging on O_2 and N_2 transport properties of thin glassy poly(arylene ether ketone) copolymer films based on tetramethyl bisphenol A and 4,4'-difluorobenzophenone

Qiang Liu, Andrew T. Shaver, Yu Chen, Gregory Miller, Donald R. Paul, J.S. Riffle, James E. McGrath, Benny D. Freeman

Please cite this article as: Liu Q, Shaver AT, Chen Y, Miller G, Paul DR, Riffle JS, McGrath JE, Freeman BD, Effect of UV irradiation and physical aging on O_2 and N_2 transport properties of thin glassy poly(arylene ether ketone) copolymer films based on tetramethyl bisphenol A and 4,4'-difluorobenzophenone, *Polymer* (2016), doi: 10.1016/j.polymer.2016.01.075.

This is a PDF file of an unedited manuscript that has been accepted for publication. As a service to our customers we are providing this early version of the manuscript. The manuscript will undergo copyediting, typesetting, and review of the resulting proof before it is published in its final form. Please note that during the production process errors may be discovered which could affect the content, and all legal disclaimers that apply to the journal pertain.
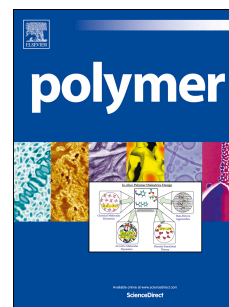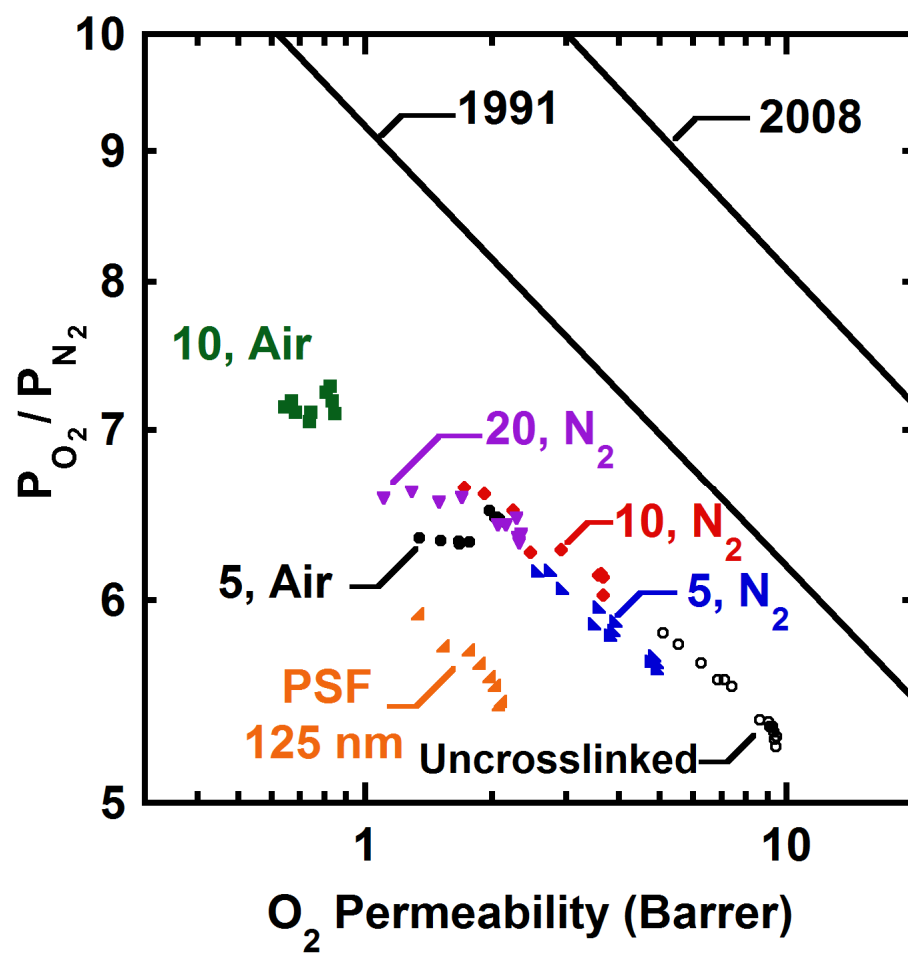
Effect of UV irradiation and physical aging on O_2 and N_2 transport properties of thin glassy poly(arylene ether ketone) copolymer films based on tetramethyl bisphenol A and 4,4'-difluorobenzophenone

Qiang Liu[1], Andrew T. Shaver[2], Yu Chen[2], Gregory Miller[2], Donald R. Paul[1],

J. S. Riffle[2], James E. McGrath[2] and Benny D. Freeman[1*]

1. Department of Chemical Engineering, Texas Materials Institute, Center for Energy and Environmental Research, The University of Texas at Austin, 10100 Burnet Road, Bldg. 133, Austin, TX 78758, USA

2. Department of Chemistry, Macromolecules and Interfaces Institute, Virginia Tech, Blacksburg, VA 24061, USA

Submission to Polymer

*Corresponding Author: Email freeman@che.utexas.edu Tel: 1-512-232-2803

Abstract

Modification of membranes to improve gas separation properties has been of considerable interest. Crosslinking is one route to modify membranes, but such studies need to be performed on thin membranes to quantify the impact of such modifications at thicknesses relevant to industrial membranes. In this study, the influences of UV irradiation and physical aging on O_2 and N_2 gas permeation properties of thin (~ 150 nm) glassy, amorphous poly(arylene ether ketone) (PAEK) copolymer films at 35 ^{o}C and 2 atm were investigated. Thin PAEK copolymer films, prepared from tetramethyl bisphenol A (TMBPA) and 4,4'-difluorobenzophenone (DFBP), were UV irradiated on both sides in air or N_2 at 254 nm or 365 nm, which induced crosslinking and, in some cases, photooxidation. Gas permeability decreased and O_2/N_2 selectivity increased as UV irradiation and aging time increased. At 254 nm, samples irradiated in air have lower permeability coefficients and higher selectivities than samples irradiated in N_2, which was ascribed to additional decreases in free volume due to photooxidation in samples irradiated in air. Additionally, samples irradiated in air at 254 nm exhibit less physical aging than uncrosslinked and samples irradiated in N_2 at 254 nm, possibly due to interactions among photooxidative polar products that may restrict polymer chain mobility, thereby lowering the aging rate. The influence of water vapor on physical aging of samples irradiated in air was examined. Finally, irradiation at 254 nm leads to more extensive crosslinking and/or photooxidation than irradiation at 365 nm, possibly due to greater UV absorption by the polymer and the higher probability of radical formation at the lower wavelength.

1. Introduction

Polymers with high permeability, high selectivity, and long term stability are desired for gas separation applications, and glassy polymers are typically used. However, the inherent non-equilibrium state of glassy polymers causes physical properties, including gas transport properties, to drift with time towards a seemingly unattainable equilibrium in a process known as physical aging [1, 2]. As polymer chains undergo self-retarding reorganization in the glassy state, polymer segmental mobility decreases due to free volume reduction [2]. Consequently, gas permeability generally decreases and selectivity increases with aging [3-5]. Several studies have demonstrated the influence of physical aging on gas transport properties of thick films (> 1 µm) [6-9]. As film thickness decreases into the range (~ 0.1 µm [10-12]) relevant for commercial gas separation membranes, gas permeability decreases more rapidly, suggesting accelerated aging in thin films [3, 13, 14]. While this phenomenon is not completely understood, it is believed to be connected to differences in polymer chain mobility at the surface versus the bulk of the films. As thickness decreases, from the tens of microns often used in initial screening of gas transport properties to 100 nm or less, surface to volume ratio increases enormously, so the influence of surface properties of such thin films on other properties (e.g., gas permeability) becomes much more important.

One route to modifying existing polymers to achieve better gas separation properties is via crosslinking. Introducing crosslinks into some polymers can improve selectivity without significant losses in permeability [15]. Crosslinking reactions may occur by either step-growth polymerization, such as reaction of an amine with an epoxy at elevated temperature [16, 17], or by chain-growth polymerization, which can be activated thermally or by irradiation, such as exposure to UV light [18, 19]. For example, Kita et al. studied the effect of UV irradiation on
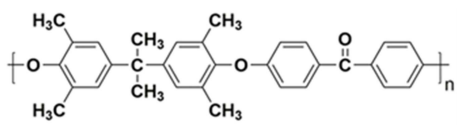
gas transport properties of a benzophenone-containing polyimide prepared from 3,3′, 4,4′-benzophenone tetracarboxylic dianhydride (BTDA) and 2,4,6-trimethyl-1,3-phenylene-diamine (TMPD) [15]. After 30 minutes of irradiation in air, the H_2/CH_4 selectivity of BTDA-TMPD increased by a factor of 50, whereas H_2 permeability decreased by a factor of only 5. Kita et al. concluded that the selectivity increase upon UV exposure was mainly due to changes in gas diffusion coefficients [15]. Similar observations were reported in a study involving polyarylates [20]. In these studies, polymer film thicknesses on the order of tens of microns were used. However, for thick aromatic polymer films absorbing significantly in the UV range, the radiation penetration depth may be small, thereby promoting crosslinking at and near the film surface but not much at the center of a film, yielding non-uniform crosslinking throughout the film [20, 21]. McCaig et al. investigated the influence of UV irradiation in N_2 and physical aging on gas transport properties of thin polyarylate films (≤ 1 µm). Both crosslinking and aging decreased gas permeability and increased selectivity, but the gain in selectivity from crosslinking was more pronounced than that due to aging. In addition, crosslinked samples exhibited slower aging than uncrosslinked samples, and this effect was attributed to the lower free volume of the crosslinked samples [22]. From a fundamental perspective, it is of interest to study uniformly irradiated samples, but the thicknesses required (<1 µm) can be in the range where physical aging effects become significant, so careful experimental design is required to separate these effects.

The irradiation environment can also influence gas transport properties. Meier et al. investigated the effect of UV irradiation in air or N_2 on permeation properties of a an uncrosslinkable polyimide [23, 24]. Pure-gas O_2/N_2 selectivity increased by 80% after the sample was irradiated in air for 30 minutes. However, the O_2/N_2 selectivity did not change after UV irradiation in N_2. FTIR analysis revealed that photooxidation products, such as hydroxyl and

carbonyl groups, formed in the sample irradiated in air, but not in the sample irradiated in N_2. Meier et al. concluded that photooxidation induced polymer densification and found polar groups at the surface. These polar groups can interact via hydrogen bonding, lower polymer free volume, and increase gas selectivity. Similar photooxidative effects were observed in other studies involving both uncrosslinkable and crosslinkable polyimides [25-27].

This study investigated the influence of UV irradiation and physical aging on gas transport properties of ultra-thin glassy, amorphous poly(arylene ether ketone) (PAEK) copolymer films ($l \sim 150$ nm) prepared from tetramethyl bisphenol A (TMBPA) and 4,4'-difluorobenzophenone (DFBP). The chemical structure and bulk properties of TMBPA-BP are presented in Table 1 [28]. This polymer was chosen because the tetramethyl substitution helps to reduce the efficiency of polymer chain packing, thereby increasing the polymer free volume and improving gas permeability and provides an abundant source of benzylic methyl groups for crosslinking reactions [29]. In addition, the benzophenone moiety is a well-known photosensitizer that can be excited upon irradiation at 250-370 nm to initiate crosslinking between polymer chains [30, 31]. The uniformity of irradiation throughout the sample depth was estimated using UV-Vis spectroscopy, and the progress of crosslinking and photooxidation was monitored using Fourier transform infrared spectroscopy (FTIR). The effects of irradiation time, irradiation environment (air vs. N_2), and irradiation wavelength (254 nm vs. 365 nm) on gas transport properties and aging behavior were explored.

Table 1. Bulk material properties (film thickness ~ 31µm) of uncrosslinked TMBPA-BP.

| Polymer | T_g (^{o}C) | Density (g/cm^3) | FFV | Permeability (Barrer)[1] | | Selectivity O_2/N_2[1] |
				O_2	N_2	
TMBPA-BP	215	1.092	0.167	4.5	0.84	5.4

[1]Gas transport properties measured at 35 ^{o}C and 10 atm.

2. Experimental

2.1. TMBPA-BP Synthesis

Sulfuric acid, acetic acid and acetone were purchased from Spectrum Chemicals (New Brunswick, NJ, USA) and used as received. N-Methyl-2-pyrrolidone (NMP) was also purchased from Spectrum Chemicals and was dried over calcium hydride and vacuum distilled before use. 4,4′-Difluorobenzophenone (DFBP) was kindly donated by Solvay and recrystallized from 2-propanol. Methylene chloride and potassium carbonate were purchased from Fisher Scientific (Pittsburgh, PA, USA). The potassium carbonate was dried at 150 ^{o}C under vacuum immediately before use. Toluene and 2,6-dimethylphenol (2,6-xylenol) were purchased from Sigma-Aldrich (St. Louis, MO, USA) and used as received.

The synthesis of tetramethyl bisphenol A (TMBPA) was adapted from the synthesis procedure for tetramethyl bisphenol F [32]. Acetone (7.103 g, 122 mmol) and 2,6-xylenol (18.92 g, 155 mmol) were added to a two-neck 250-mL round bottom flask fitted with a mechanical stirrer and an addition funnel. The solution was stirred and cooled to 15 ^{o}C in an ice bath. A solution of sulfuric acid (16.304 g, 0.163 mol) and acetic acid (17.392 g, 0.290 mol) was

mixed, chilled to 15 ^{o}C, and added dropwise to the reaction flask via the addition funnel. The reaction mixture was maintained at room temperature overnight, diluted with 100 mL of water and 150 mL of methylene chloride, and then transferred to a separatory funnel. The organic layer was washed with deionized water three times before collection. The methylene chloride layer was dried over magnesium sulfate overnight and then evaporated to yield the crude product. The product was recrystallized from toluene. Yield was 70%. The melting point of the recrystallized product was in good agreement with the reported value (162 ^{o}C) [33].

TMBPA (29.362 g, 103.2 mmol) and DFBP (22.527 g, 103.2 mmol) were added to a three-neck 500 mL round bottom flask equipped with a mechanical stirrer, a condenser, a nitrogen inlet and a Dean-Stark trap. NMP (300 mL) was added to the flask, and the mixture was stirred to obtain a clear solution. Afterwards, K_2CO_3 (16.408 g, 118.7 mmol) was added, followed by 150 mL of toluene. The reaction bath was heated at 155 ^{o}C for 4 h to remove the water and toluene, kept at 150 ^{o}C for 12 h, and then cooled to room temperature. The reaction mixture was filtered to remove any excess K_2CO_3 or by-product salts and precipitated in 1000 mL of deionized water. The resulting polymer was stirred in deionized water at 80 ^{o}C overnight and then dried under vacuum at 110 ^{o}C for at least 48 h. The yield of TMBPA-BP was 81%. At 35 ^{o}C, which is the temperature used for both aging and permeation experiments in this study, TMBPA-BP is deep within its glassy state (about 180 ^{o}C below its T_g, as shown in Table 1).

2.2. Film preparation

In general, to avoid rapid evaporation of solvent during spin coating, solvents with high boiling points (>100 ^{o}C) and low vapor pressures are preferred [3, 4, 34]. For this reason, toluene was used in this study. Film thickness was controlled by varying the solution

concentration, typically between 2 and 3 wt%. About 15 mL of polymer solution was prepared and filtered through 5 µm, 0.45 µm, and 0.1 µm Puradisk[TM] PTFE syringe filters (Whatman, Pittsburg, PA, USA), in that order, to remove dust or particulates. Afterwards, the solution was sonicated for 30 min to remove dissolved air bubbles, since air bubbles can introduce pinhole defects in thin films [34].

Thin films were prepared by spin coating the polymer solution onto silicon wafers (Nova Electronics Materials, Flower Mound, TX, USA) at 1000 rpm for 3 min. Next, the silicon wafer was placed on a hot plate and heated at 130 $^\circ$C for 3 min to remove residual solvent. To avoid dust and particulates in the environment, spin coating was performed inside a class 100 clean room. Film thickness was measured using a variable angle spectroscopic ellipsometer (VASE) (M2000D, J. A. Woollam Co., Lincoln, NE, USA). Psi (ψ) and delta (Δ) parameters were taken at three different angles (65, 70, and 75 degrees) over a wavelength range of 450 – 1000 nm, and the data was modeled using the Cauchy equation [4, 12, 14, 34].

A challenge in fabricating sub-micron films is to avoid the presence of pinhole defects, which compromise gas selectivity and render the film useless for gas separation characterization [14, 35]. To mitigate this problem, a second layer of highly permeable polymer, such as PDMS, is often coated onto the selective layer to block the pinholes and, thus, the selectivity-destroying convective flow [14, 36-38]. This practice of "caulking" the defects was initially employed in industry to treat hollow fiber membranes [36-39], and recently was used to study the influence of physical aging on gas transport properties of ultra-thin (< 400 nm) films [12, 14, 35, 40]. At the aging temperature used for this study, PDMS is about 150 $^\circ$C above its T_g [14], and therefore, will not undergo physical aging [13, 14]. In addition, the PDMS layer, with a thickness typically in the range of 5-6 µm, can also provide mechanical support to the very thin selective layer.

Rowe et al. [14] and Cui et al. [12] demonstrated that PDMS did not significantly change the gas transport properties of the thin glassy polymers they considered, so we presume that it does not influence the permeability of the glassy polymers considered in this study.

A PDMS solution was prepared by mixing Wacker Silicones Corporation Dehesive 944 and cyclohexane in a 2:3 ratio by mass and then adding a crosslinking agent (V24) and proprietary catalyst (OL) as described elsewhere [34, 35]. After the glassy polymer thickness was measured using an ellipsometer, the PDMS/cyclohexane solution was spun onto the glassy polymer at 1000 rpm for 1 min. The wafer was then heated to 115 ^{o}C for 15 min to fully crosslink the PDMS. The PDMS layer thickness was measured using a Dektak 6M stylus profilometer (Veeco, Plainview, NY, USA).

The bilayer film was lifted from the wafer using deionized water and transferred to a thin rectangular loop of copper wire (Cat# 2781345, Radio Shack, Austin, TX, USA). The free-standing thin film was then annealed at 233 ^{o}C (~ 15 ^{o}C above T_g) for 5 min in an HP 5890 gas chromatograph (GC) oven under an ultra-high purity nitrogen purge to erase thermal history and any orientation effects [4]. The start of the aging process (t = 0) is defined as the time when the thin film was removed from the GC oven and rapidly quenched to ambient conditions.

2.3 UV-Vis Spectroscopy

Ultraviolet-visible spectroscopy (UV-Vis) was performed using an Agilent Cary 5000 UV-Vis-NIR spectrophotometer (Santa Clara, CA, USA). Free-standing films were attached to a sample holder and covered an aperture through which light at various wavelengths passed. Absorbance was measured at wavelengths ranging from 200-800 nm at a scan rate of 600 nm/min.

2.4 FTIR

FTIR was performed using a Thermo Nicolet 6700 spectrometer (Waltham, MA, USA) equipped with a DTGS detector. Samples were tested in transmission mode with a resolution of 4 cm^{-1} and 256 scans per sample.

2.5 UV irradiation

Thin film samples were irradiated in air or N_2 for various amounts of time on each side using either a UV crosslinker (XL-1000, Spectronics, Westbury, NY, USA) equipped with 254 nm light filter bulbs or a 100W high pressure mercury arc UV lamp (Blak-Ray B-100, UVP, Upland, CA, USA) equipped with a 365 nm light filter bulb. Samples were placed 12 cm from the bulbs in the UV crosslinker and 4 cm from the bulb of the UV lamp. The UV intensity at the film surface was monitored using a radiometer (Part# 97-0015-02, UVP, Upland, CA, USA) and was found to be 6.55 mW/cm^2 at 254 nm and 16.7 mW/cm^2 at 365 nm. For irradiation in N_2, both the crosslinker and the UV lamp were placed inside a glove box (Cat# 50601-00, Labconco, Kansas City, MO, USA). Prior to UV irradiation, the glove box was purged with N_2 (UHP grade, Airgas, Austin, TX, USA) until the O_2 level was below 0.1% by volume, which was monitored using an oxygen sensor (Part# 9452, Nuvair, Oxnard, CA, USA). At 254 nm, films were irradiated up to 10 min (5 min per side) in air and 20 min (10 min per side) in N_2. Samples irradiated for longer times were not mechanically stable for subsequent characterization experiments. At 365 nm, films were irradiated for 10 min (5 min per side) in air or N_2.

2.6 Gas permeation

The influence of physical aging (up to approximately 1000 hours) on O_2 and N_2 permeation properties of uncrosslinked and UV-irradiated thin films was investigated. Permeability coefficients were measured at 35 ^{o}C and an upstream pressure of 2 atm using a constant-volume, variable-pressure permeation apparatus built in house [41]. Thin films were supported on a 0.02 µm AnoPore membrane disc (Cat# 6809-5502, Whatman, Maidstone, England) and masked on both sides with aluminum tape, as described previously [35]. The mass transfer resistance from the PDMS layer can be accounted for using a series resistance model as follows [14, 42]:

$$\frac{l_{composite}}{P_{composite}} = \frac{l_{PDMS}}{P_{PDMS}} + \frac{l_{Glassy}}{P_{Glassy}} \qquad (1)$$

where l_{PDMS}, l_{Glassy}, and $l_{composite}$ are the thicknesses of the PDMS layer, the underlying selective layer, and the overall composite ($l_{PDMS} + l_{Glassy}$), respectively. Accordingly, P_{PDMS}, P_{Glassy}, and $P_{composite}$ are the permeability coefficients of PDMS, the glassy polymer, and the composite structure, respectively. Permeability coefficients of gases in PDMS do not change with time, and these permeability coefficients were obtained from the literature [14]. Permeability of gases in both the uncrosslinked and UV-irradiated TMBPA-BP thin films was calculated using Equation (1). When polymer samples were not installed in the gas permeation systems for permeation experiments, they were shielded from light and allowed to age inside a dark gas chromatograph (GC) oven at 35 ^{o}C.

3. Results and discussion

3.1 UV irradiation uniformity

One general question of interest in UV crosslinking is the crosslinking uniformity through the sample. In the thin films considered in this study, we cannot directly measure the extent of crosslinking as a function of depth into the sample. However, we can estimate the uniformity of UV irradiation throughout the sample. Presumably, more uniform irradiation throughout the sample will contribute to more uniform crosslinking. The UV intensity at any point in a film, *I*, can be estimated using the Beer-Lambert law [20]:

$$I = I_0 \times 10^{-ECD} = I_0 \times 10^{-A} \qquad (2)$$

where I_0 is the incident UV intensity, E is the extinction coefficient, C is the concentration of photoactive species in the film, D is the path length, and A is the absorbance. As UV irradiation penetrates deeper into these aromatic polymer films, its intensity will decrease due to absorption of light by the polymer. If there is a sharp gradient of UV intensity between the surface and the center of a film, the resulting crosslinking may not be uniform. For such a non-uniform crosslinked material, the measured gas permeability would not represent the intrinsic property of a homogeneously crosslinked polymer and, therefore, could not be directly compared with the permeability of uncrosslinked samples or other non-uniform crosslinked samples.

Fig. 1A presents the UV-VIS spectra of TMBPA-BP films of different thicknesses. A strong band at ~200 nm represents the π→π* transition associated with the benzophenone excitation, and a weaker band at ~280 nm represents the n→π* transition [30]. As film thickness decreases, the absorbance at 254 nm (i.e., one of the crosslinking wavelengths considered) decreases. Because the product EC in Equation (2) is a material property and is, therefore,

independent of film thickness, absorbance should be linearly correlated with film thickness, as shown in Fig. 1B. Using Equation (2), relative UV intensity at any depth in a film can be calculated. Fig. 1C shows a calculated profile of relative UV intensity for TMBPA-BP films of different thicknesses. Normalized film thickness values of 0 and 1 correspond to the two surfaces of a film. Because each film was irradiated for the same amount of time on each side, the calculated UV intensity profile has a parabolic shape. To increase the uniformity of an irradiated sample, the film needs to be thin enough so that the UV intensity at the center of the film is as similar as possible to that at the surface. As shown in Fig. 1C, the profile becomes more uniform as film thickness decreases. For example, for a 259 nm TMBPA-BP film, there is a 32% difference between the UV intensity at the surface and the center of the film. For a 145 nm film, there is only a 14% difference between the UV intensity at the surface and the center of the film. Hypothetically, films thinner than 145 nm would have an even more uniform irradiation, but to consistently make defect-free films at such thicknesses is very difficult. As a result, films of around 145 nm were used for this study to balance the competing needs for relatively uniform irradiation and the practicality of making very thin, defect-free films.
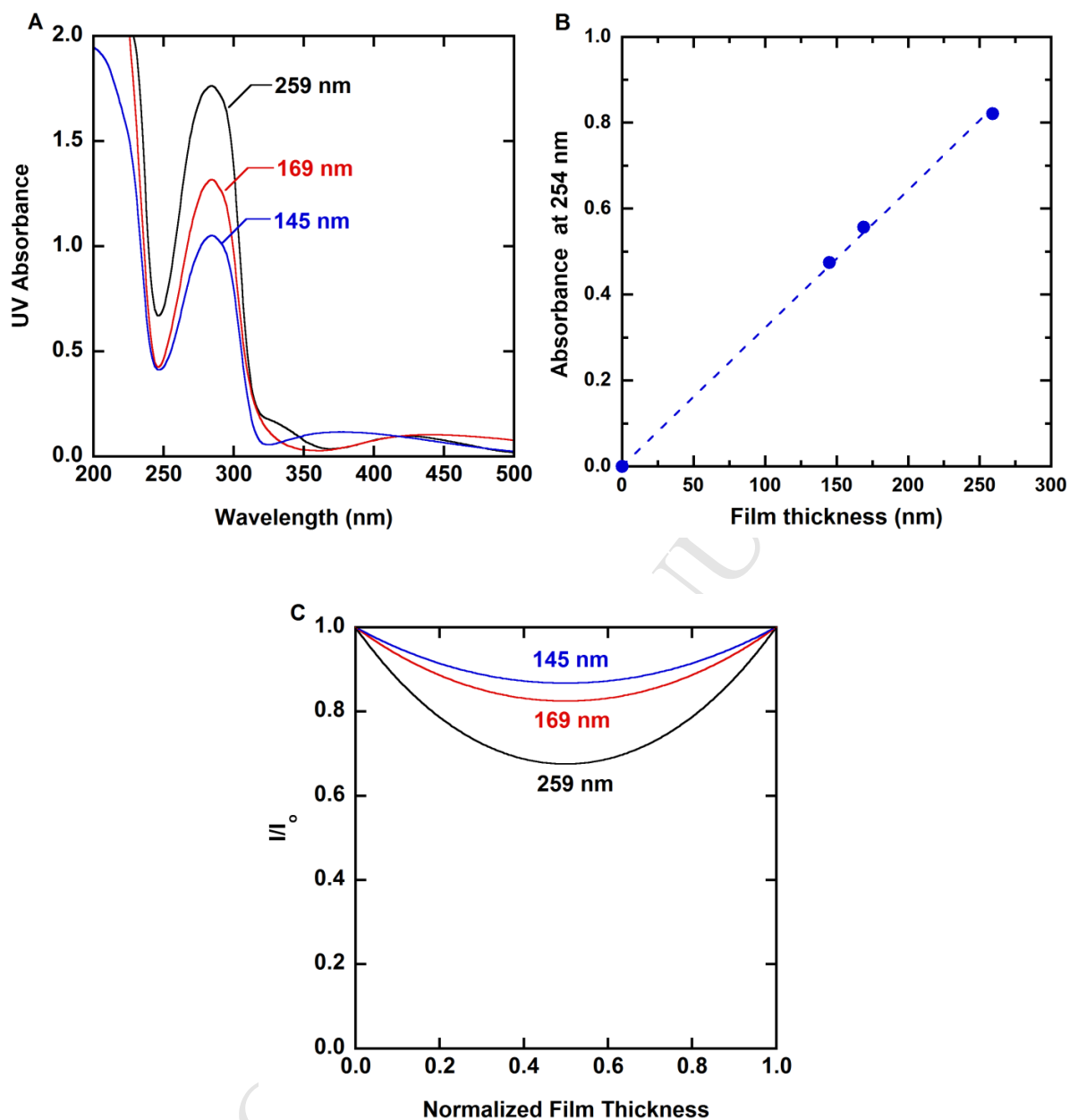
Fig. 1. (A) Effect of film thickness on UV-Vis spectra of TMBPA-BP films. (B) Effect of film thickness on UV absorbance at 254 nm. (C) Calculated UV intensity profile at 254 nm in TMBPA-BP films of various thicknesses.

Because PDMS is coated onto the glassy polymer to prevent pinholes from affecting the

transport results, one question is whether the PDMS layer may significantly shield the UV light

from the underlying glassy polymer, thereby affecting the irradiation uniformity in the glassy polymer. Fig. 2A presents the UV-Vis spectrum of a TMBPA-BP film (l=145 nm) and a crosslinked PDMS film (l = 6 µm). The absorbance for PDMS is very low at wavelengths above 250 nm. At an irradiation wavelength of 254 nm, the PDMS absorbance (0.069) is 85% lower than that of the TMBPA-BP thin film (0.475). Fig. 2B presents the calculated UV intensity profile at 254 nm for TMBPA-BP films with or without PDMS coating. Because the PDMS coating is applied to only one side of the film (at a normalized film thickness = 1 in Fig. 2B), the addition of PDMS skews the UV profile slightly away from the center. The maximum difference in UV intensity between the film surface and the interior is 14% for the TMBPA-BP film without a PDMS coating and 17% for the film with a PDMS coating. Therefore, the influence of the PDMS layer on UV irradiation uniformity is believed to be small.
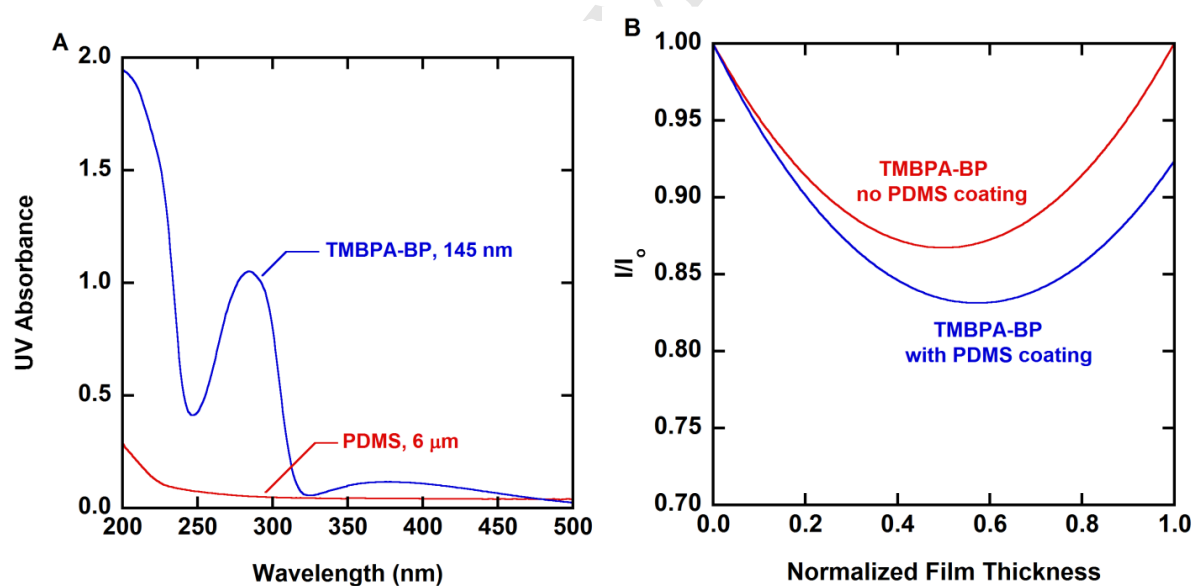

Fig. 2. (A) UV-Vis spectra for TMBPA-BP and PDMS. (B) Calculated UV intensity profile at 254 nm in TMBPA-BP films (l = 145 nm) with and without a PDMS coating.

Additionally, UV treatment at 254 nm and 365 nm is not expected to change the physical and gas transport properties of PDMS. PDMS is generally stable against UV irradiation at wavelengths above 200 nm [43, 44]. Below 200 nm, UV irradiation in air can promote ozone formation, which may induce polymer chain scission and oxidation of PDMS to SiO_2 at the polymer-air interface, thereby affecting PDMS physical properties [44-46]. However, at the wavelengths considered in this study (i.e., 254 nm and 365 nm), UV absorbance in PDMS is small (cf., Fig. 2A). Because light must be absorbed for photochemical reactions to occur (i.e., the Grotthuss-Draper law) [47], little photochemical activity, and thereby physical property changes, are expected at 254 nm and 365 nm.

Because UV absorbance at 365 nm is much lower than that at 254 nm (cf., Fig. 1A), irradiation at 365 nm is more uniform than at 254 nm. For example, the absorbance of a 145 nm thick TMBPA-BP film at 365 nm (0.112) is 76% lower than that at 254 nm (0.475). As a result, at 365 nm, the difference between the UV intensity at the surface and center of a 145 nm thick film is less than 1%, resulting in a relatively uniformly irradiated sample.

3.2 Crosslinking and photooxidation

Crosslinking and photooxidation reactions via UV irradiation of benzophenone-containing polymers have been reported [23, 24, 48]. Based upon previous studies, Fig. 3 presents several reaction pathways that may occur to various extents. Upon irradiation at 250-370 nm, benzophenone (BP) can be excited and abstract a labile hydrogen to yield carbon-centered radicals and benzylic radicals (reaction 1). If oxygen is present, benzylic radicals (**D**) can react with oxygen to form peroxy radicals (**E**), which can then abstract another hydrogen to

form peroxides (**F**). Further UV irradiation and subsequent hydrogen abstraction decompose the

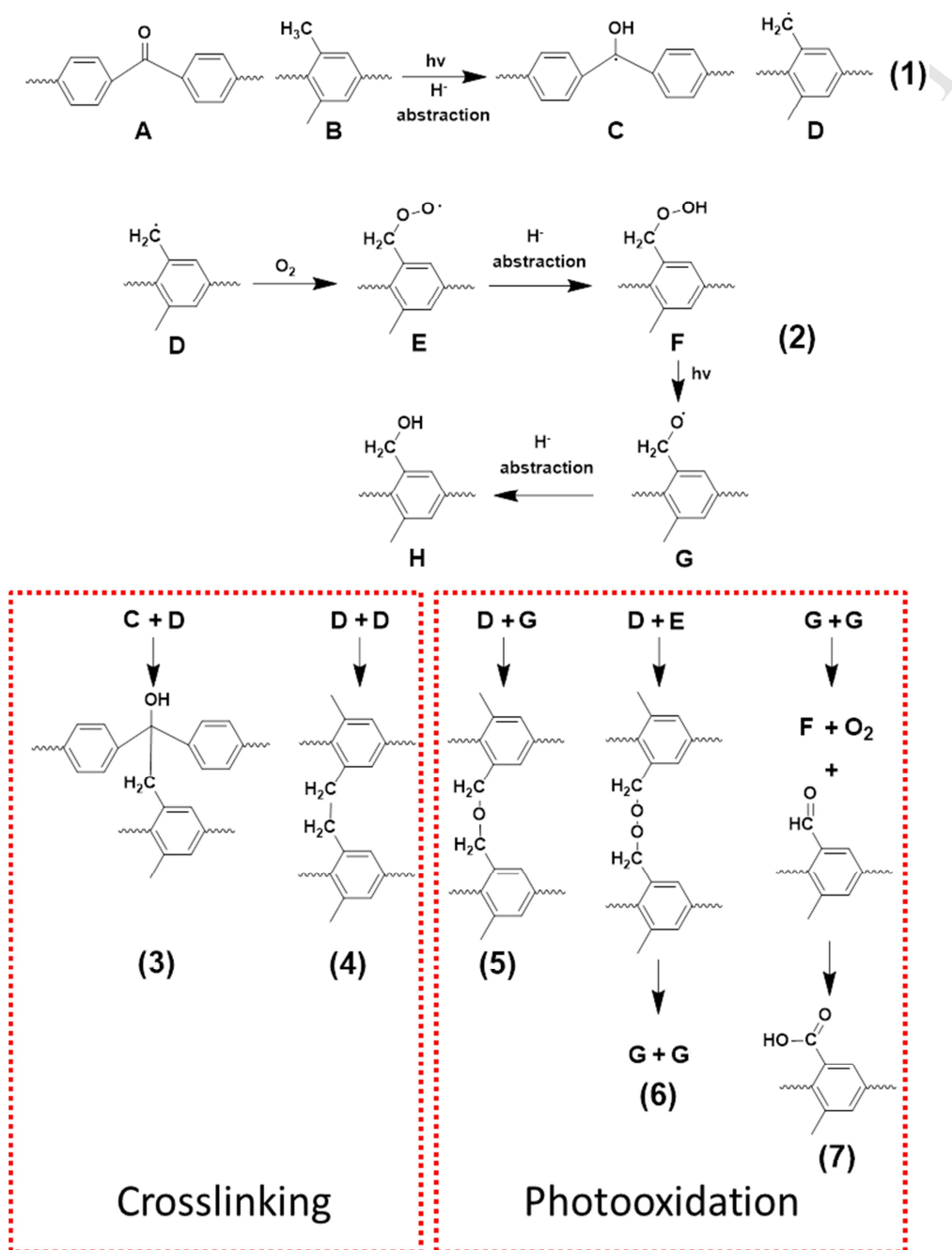peroxides to generate alkoxy radicals (**G**) and hydroxides (**H**) (reaction 2).

Fig. 3. Expected mechanism of UV-induced crosslinking and photooxidation [23, 24, 48].

Radicals can couple according to either the crosslinking or photooxidation pathways, as outlined in Fig. 3. For crosslinking reactions, benzylic radicals can couple with carbon-centered radicals derived from the benzophenone (reaction 3) or benzylic radicals (reaction 4) to form crosslinks between polymer chains. McCaig et al. speculated, based on CPK models, that steric hindrance might limit the benzylic-carbon radical coupling (reaction 3) [22], although this has not been proven.

Photooxidation reactions can occur via coupling of oxidized intermediates, according to reactions 5-7. For example, benzylic radicals (**D**) can couple with either alkoxy (**G**) or peroxy (**E**) radicals to form aliphatic ethers (reaction 5) or peroxides (reaction 6), respectively. However, because peroxides are typically not stable, they tend to rapidly dissociate to yield more alkoxy radicals (reaction 6). Finally, alkoxy radicals (**G**) can couple with other alkoxy radicals (**G**) to form aldehydes, which can be subsequently oxidized to carboxylic acids (reaction 7). Interactions among these polar groups, e.g., hydrogen bonding, etc., can potentially increase interchain cohesion, thereby decreasing polymer free volume and increasing gas selectivity [24].

3.3 FTIR characterization

Figs 4A-4C present FTIR spectra of TMBPA-BP films before and after UV irradiation under different conditions. It is noted that while these films were too thin to be able to accurately measure gel fractions on the irradiated samples, none of the irradiated materials dissolved in chloroform or appeared to swell significantly. The peak at around 1650 cm^{-1} corresponds to the carbonyl group in the benzophenone moiety, and the peak near 1600 cm^{-1} is attributed to the stretching of substituted benzene moieties [48, 49]. The intensity of each spectrum was normalized using the peak at 1600 cm^{-1} as an internal reference, which was

assumed to remain unchanged with UV irradiation. As shown in Fig. 4A and 4B, the carbonyl peak intensity at 1650 cm^{-1} decreases with increasing UV irradiation time. Concomitantly, a broad band at around 3500 cm^{-1}, attributed to the stretching of hydroxyl groups generated via crosslinking and/or photooxidation [25, 49], forms and increases with increasing UV irradiation time. In the spectra of samples irradiated in air at 254 nm (Fig. 4A and 4C), a broad absorption at ~1730 cm^{-1}, which is attributed to C=O stretching from aldehydes and carboxylic acids generated from photooxidation, emerges and increases in intensity with increasing irradiation time. Interestingly, this band was also observed in the spectra of certain samples irradiated in N_2 (e.g., "20, N_2", Fig. 4B). As described in the Experimental section, the glove box was purged with N_2 until the O_2 level was below 0.1% by volume. Thus, low levels of residual oxygen in the predominantly N_2 atmosphere might have caused low levels of photooxidation, especially for samples irradiated for relatively long times. Interestingly, as shown in Fig. 4C, samples irradiated in air and N_2 at 365 nm have similar IR spectra to the uncrosslinked sample, suggesting that the irradiation dose at 365 nm may not have been sufficient to cause significant crosslinking or photooxidation for the irradiation times considered.
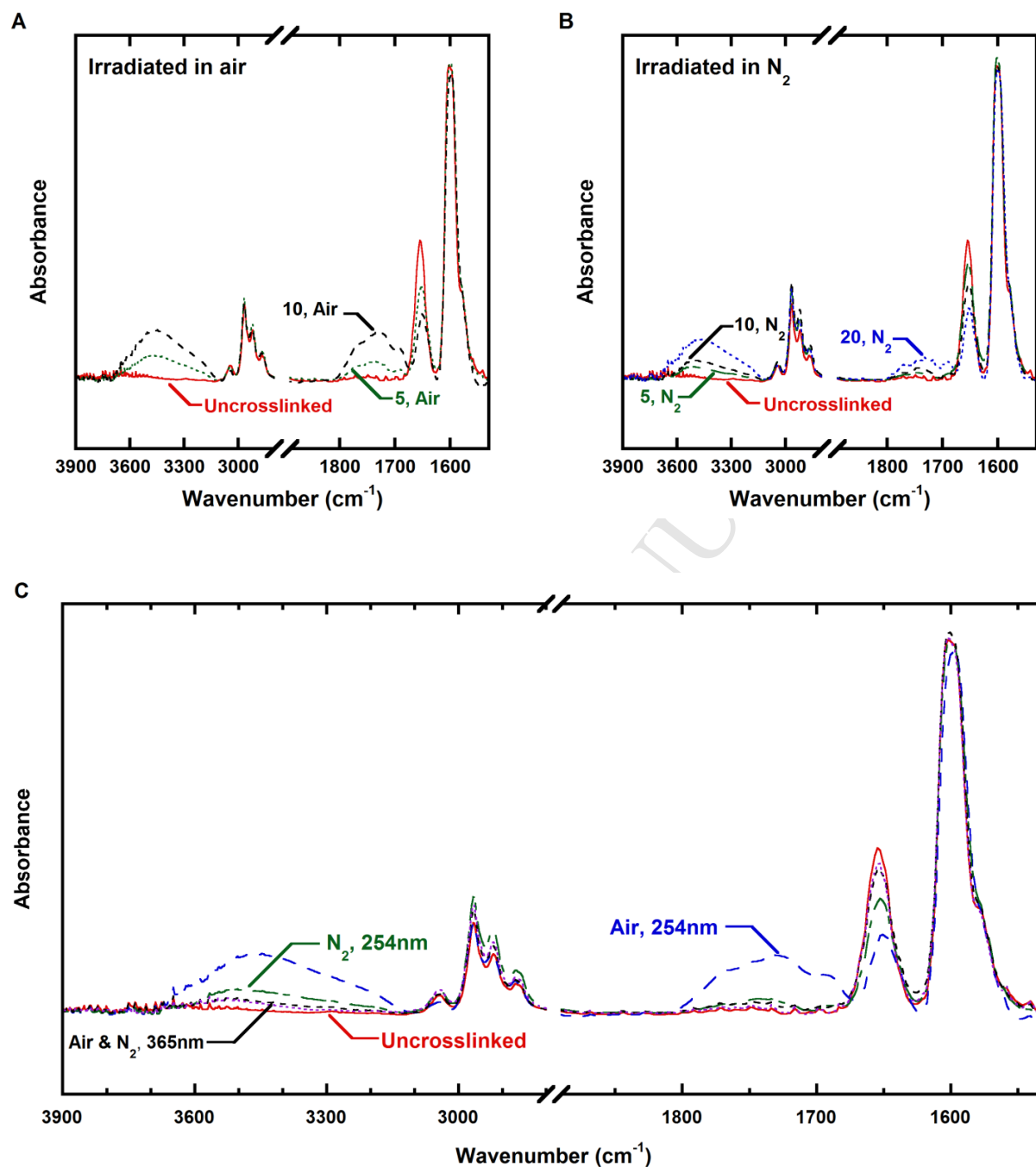
Fig. 4. FTIR spectra of TMBPA-BP films before and after UV irradiation. Samples in (A) and (B) were irradiated at 254 nm and are designated by the total irradiation time (in min) and the irradiation environment. Samples in (C) were irradiated for 10 min (5 min/side) and are designated by the irradiation environment and irradiation wavelength. All samples were 150-170 nm thick.

The progress of crosslinking and/or photooxidation can be monitored by observing the decrease in the benzophenone ketone absorption (1650 cm^{-1}) in the FTIR spectra with irradiation. Fig. 5 presents the relative BP absorption as a function of irradiation time. The relative amount of absorption at 1650 cm^{-1} was calculated by dividing the BP absorption of irradiated samples by that of an uncrosslinked sample. Because variations in sample thickness were small (< 10%), they are not expected to significantly affect the FTIR absorption intensities. As irradiation time and energy increase, the relative BP absorption decreases as BP undergoes excitation and forms crosslinks or photooxidation products. Samples irradiated in air undergo photooxidation in addition to crosslinking, so they experience a greater reduction in BP absorption than samples irradiated in N$_2$. For example, after irradiation at 254 nm for 10 min, the relative BP intensity of a sample irradiated in air is 33% lower than that of a sample irradiated in N$_2$.
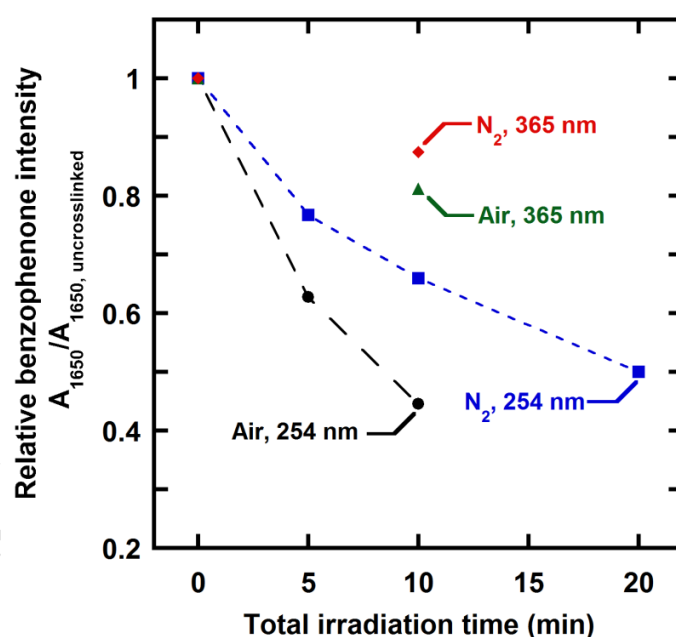

Fig. 5. Relative FTIR intensities of the benzophenone peak at 1650 cm^{-1} as a function of total irradiation time, irradiation wavelength, and irradiation environment.

As shown in Fig. 5, for a fixed irradiation environment and exposure, irradiation at 254 nm results in lower BP intensities than at 365 nm, so UV irradiation at 254 nm may cause a greater extent of crosslinking and/or photooxidation than irradiation at 365 nm. In general, the amount of radicals generated via UV irradiation depends on the amount of UV energy absorbed by the polymer and the efficiency of the absorbed energy to form radicals [18, 50]. Table 2 characterizes the different UV irradiation methods considered in this study. After undergoing irradiation for 10 min, polymers irradiated at 254 nm absorbed more energy per unit area than those irradiated at 365 nm. Moreover, because photons at 254 nm (472 kJ/mol) are more energetic than those at 365 nm (328 kJ/mol), photons at 254 nm are more likely to overcome the energy barrier (310 kJ/mol) required to promote the n→π* transition of benzophenone (cf., Fig. 1) [51, 52], which leads to more radicals available for photochemical reaction. Consequently, due to greater UV energy absorption and a higher probability of radical formation, irradiation at 254 nm may lead to more crosslinking and/or photooxidation than irradiation at 365 nm.

Table 2. Characteristics of UV irradiation methods at 254 nm and 365 nm. Films are typically 150-170 nm thick.

	Irradiation at 254 nm	Irradiation at 365 nm
Absorbance[a]	0.475	0.112
UV intensity (mW/cm^2)	6.55	16.7
Emitted energy per area after 10 min irradiation (mJ/cm^2)	3900	10,000
Absorbed energy per area after 10 min irradiation (mJ/cm^2)[b]	2600	2300
Irradiation dose After 10 min irradiation (kGy)[c]	1.6×10^5	1.4×10^5

[a] cf., Fig. 1

[b] determined using Equation (2)

[c] estimated using the film thickness and the bulk film density (cf., Fig. 1), $1 kGy = 1$ kJ absorbed/kg of polymer

3.4 Influence of irradiation time and environment on physical aging and gas transport properties

Fig. 6 presents O_2 permeability (Fig. 6A) and relative O_2 permeability (Fig. 6B) as a function of aging time for uncrosslinked and irradiated TMBPA-BP films with thicknesses ranging from 150 to 170 nm. The relative O_2 permeability was calculated by dividing the O_2 permeability coefficient (P) at a given aging time by its initial value (P_0) at about 1 h of aging, which was the time at which the first permeation measurement could be conducted. The films were irradiated at 254 nm, and they are designated by the total irradiation time and environment. For example, "20, N_2" indicates a sample irradiated in N_2 at 254 nm for 20 min (10 min/side). The initial O_2 permeability of the uncrosslinked thin film is higher than that of the bulk film (cf., Table 1), indicating that additional free volume may have been captured in the thin film due to

rapid quenching from above T_g [3, 13, 14, 22]. As aging time increases, free volume of glassy polymers typically decreases [4], leading to permeability decreases. For example, the O_2 permeability of the uncrosslinked sample decreases by almost 50% after about 1000 h of aging.
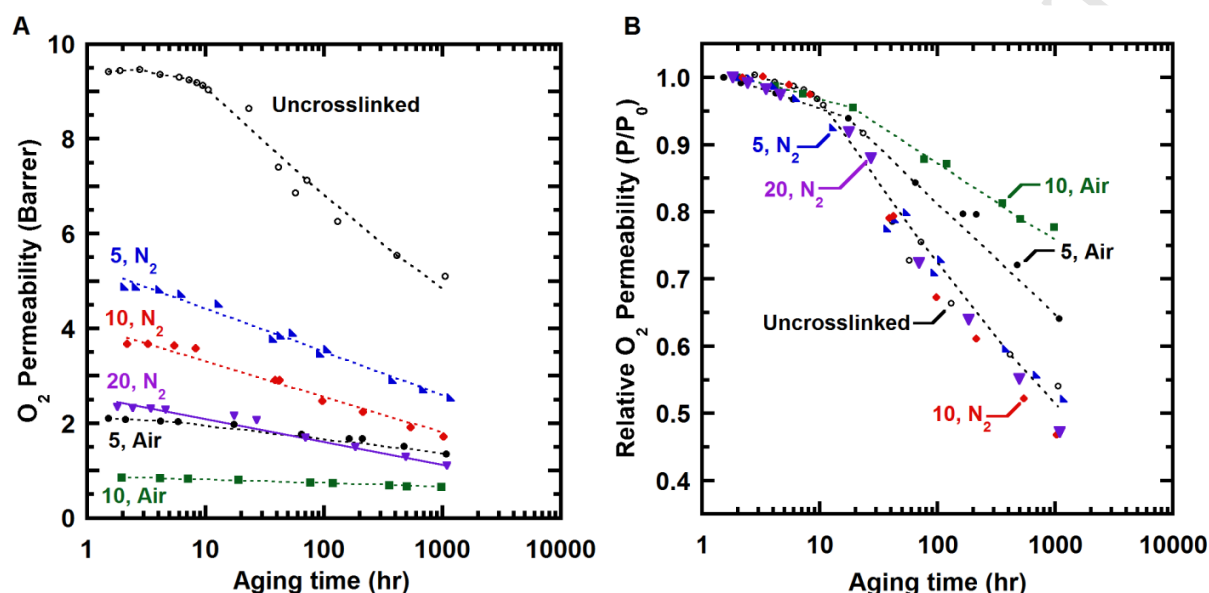

Fig. 6. Influence of physical aging on: (A) oxygen permeability and (B) normalized oxygen permeability of uncrosslinked and irradiated TMBPA-BP films. In (B), relative O_2 permeability was calculated by dividing the O_2 permeability (P) at a given aging time by its initial value (P_0) at ~ 1 h of aging time. Samples were irradiated at 254 nm, and they are designated by the total time (in min) and the environment of UV irradiation. Lines are drawn to guide the eye.

The oxygen permeability also decreases with UV irradiation in either N_2 or air, which may be due to a loss in polymer free volume with crosslinking and/or photooxidation [22, 25]. Interestingly, as shown in Fig. 6B, samples irradiated in N_2 display similar rates of permeability loss as that of the uncrosslinked sample. Materials having different permeability coefficients yet similar aging rates have been reported in earlier studies [3, 5, 53]. For example, Kim et al. observed that a chemically crosslinked thin polyimide film (281 nm thick) had a similar aging rate as its uncrosslinked analog (312 nm thick), even though the initial O_2 permeability of the

crosslinked sample was 57% lower than that of the uncrosslinked film [53]. Similar observations were also reported for thin films of polysulfone (annealed vs. non-annealed) [5] and poly(2,6-dimethyl-1,4-phenylene oxide) (semicrystalline vs. amorphous) [3].

The aging rate, according to the self-retarding aging model developed by Struik, can be expressed as the ratio of the driving force, i.e., the displacement of the specific volume at time t away from that at equilibrium, to a characteristic relaxation time, τ, which is a function of the polymer's current free volume state, glass transition temperature, T_g, and experimental temperature [2]:

$$\text{Aging rate} \equiv \frac{dv}{dt} = \frac{-(v-v_\infty)}{\tau\,(v,T_g-T)} \tag{3}$$

where v and v_∞ are the specific volumes of the polymer at time t and at equilibrium, respectively. One possible explanation for the similar aging rates of the uncrosslinked and samples irradiated in N_2 is that the decrease in polymer free volume due to crosslinking may not be significant enough to considerably decrease the driving force, (i.e., lower $v - v_\infty$), for aging. In addition, the distance between crosslinks in samples irradiated in N_2 may be large enough that local polymer segmental mobility is not significantly restricted by crosslinking, leading to small changes in relaxation time (i.e., higher τ). The net effect of these factors (i.e., lower $v - v_\infty$ and higher τ) should reduce the aging rate (cf., Equation (3)). However, because samples irradiated in N_2 and the uncrosslinked polymer exhibit similar aging rates, the changes to the driving force and the relaxation time are likely minor.

For a fixed UV irradiation time, samples irradiated in air have lower O_2 permeability than samples irradiated in N_2. In addition to crosslinking, photooxidation can occur due to irradiation

in air, which introduces polar groups into the polymer matrix (cf., Fig. 4B). Interactions among these polar groups, such as hydrogen bonding, etc., can increase interchain cohesion, thereby lowering free volume and gas permeability [23, 24]. Moreover, such interactions may also restrict polymer chain mobility, increasing T_g, and according to Equation (3), increase the relaxation time, thereby decreasing the aging rate. Consistent with this hypothesis, as shown in Fig. 6B, samples irradiated in air have lower aging rates than uncrosslinked polymer and samples irradiated in N_2, and the aging rate of samples irradiated in air decreases as irradiation time increases.

In addition to the interactions described above, polar groups introduced by photooxidation can potentially increase polymer hydrophilicity [54]. Particularly in more hydrophilic polymers, water can influence physical aging [55]. To explore the potential influence of water on physical aging of polymers irradiated in air considered in this study, two fresh thin film samples were prepared and irradiated in air for 10 min (5 min/side). One film was kept in a permeation apparatus for up to 1000 hours. Except during permeation measurements, which used dry O_2 and N_2, that film was aged in vacuum at 35 ^{o}C and, consequently, had minimal contact with water vapor. The other sample was aged in a dark GC, which had a relative humidity of about 25%, at 35 ^{o}C. The relative humidity was measured using a VWR electronic digital humidity meter (P/N 35519-055, VWR, Radnor, PA, USA). After each permeation measurement, the sample was immediately removed from the permeation apparatus and continued aging in the ambient atmosphere. The aging behavior of these samples is presented in Fig. 7. During the first 21 h, each sample was kept in its respective permeation apparatus, so the samples were not exposed to water vapor, and the initial change in relative O_2 permeability with time is essentially identical for both samples. After about 21 h, one sample

was removed from its permeation system and aged in the ambient environment, as described above. As shown in Fig. 7, the sample aged in the ambient environment, which contained water vapor at about 25% relative humidity, underwent accelerated aging relative to the sample aged in vacuum, which were not exposed to water.
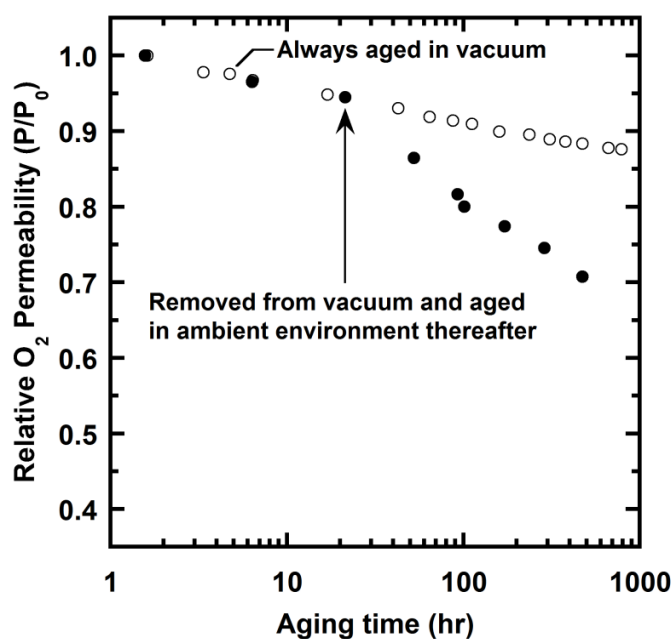

Fig. 7. Influence of aging environment on aging rate of TMBPA-BP thin films irradiated in air. Relative O_2 permeability was calculated by dividing the O_2 permeability (P) at a given aging time by its initial value (P_0) at ~ 1 h of aging time. The films were irradiated in air for 10 min (5 min/side) and were around 170 nm thick. One sample was aged in vacuum at 35 ^{o}C, and the other sample was aged in vacuum for 21 hours before being subsequently aged in the ambient environment, which had a relative humidity of about 25%, at 35 ^{o}C.

This accelerated aging in the presence of water is similar to a phenomenon reported by Horn et al., who investigated the influence of long term CO_2 exposure on aging behavior of thin Matrimid films (~200 nm) [35]. At a fixed feed pressure and temperature, CO_2 permeability in Matrimid initially increases with increasing aging time until a maximum is reached, then it decreases for the remainder of the experiment. Initially, CO_2 plasticizes the polymer and

increases gas permeability. Then, once the polymer is plasticized, its free volume increases and T_g decreases, leading to an increase in the driving force for physical aging and a decrease in the relaxation time (cf., Equation (3)), both of which act to increase the aging rate. Consequently, at later times, the influence of aging on permeability becomes more important than the initial plasticization/swelling event, resulting in a decrease in CO_2 permeability with time [35, 56]. A similar interplay between plasticization and physical aging may also be at work in this study. Because water ($T_c = 647$ K [57]) is much more condensable than CO_2 ($T_c = 304$ K [57]), water can potentially plasticize the more hydrophilic samples irradiated in air, leading to accelerated aging, as shown in Fig. 7. Of course, other components in the ambient environment, such as carbon dioxide or other species, may also have an impact on physical aging. A more detailed and controlled study of aging environment influence on aging behavior deserves further investigation, but it is beyond the scope of this study. In any case, the observed dependence of aging rate on the aging environment highlights the importance of maintaining consistent aging conditions and reporting how samples are stored between gas permeation measurements during aging studies.

Fig. 8 presents the absolute (A) and relative (B) O_2/N_2 selectivity of uncrosslinked and irradiated samples as a function of aging time. Relative selectivity was determined by dividing selectivity at time t by the initial selectivity, which was measured after about 1 h of aging. The uncertainty for the 10 min, air-irradiated sample is presented, calculated based on uncertainties in permeability coefficients using propagation of errors [58]. Uncertainties in the other data points are believed to be similar, but they are not shown for clarity in this figure. The initial O_2/N_2 selectivity of the uncrosslinked sample is similar to that of the bulk film (cf., Table 1), indicating that the PDMS-coated thin film is essentially defect-free. Selectivity generally increases with

irradiation time and aging time. This increase in selectivity can be attributed to potential densification of the polymer accompanying UV irradiation and physical aging, which should reduce the free volume and increase the size-sieving ability of the polymer [22]. At fixed irradiation time, samples irradiated in air have higher O_2/N_2 selectivity than samples irradiated in N_2. As mentioned earlier, samples irradiated in air undergo both crosslinking and photooxidation, which can effectively lower polymer free volume, restrict chain mobility, and improve selectivity [15, 23, 26]. As a result of lower aging rates of samples irradiated in air (cf., Fig. 6B), the O_2/N_2 selectivities of these samples do not change much with aging time.
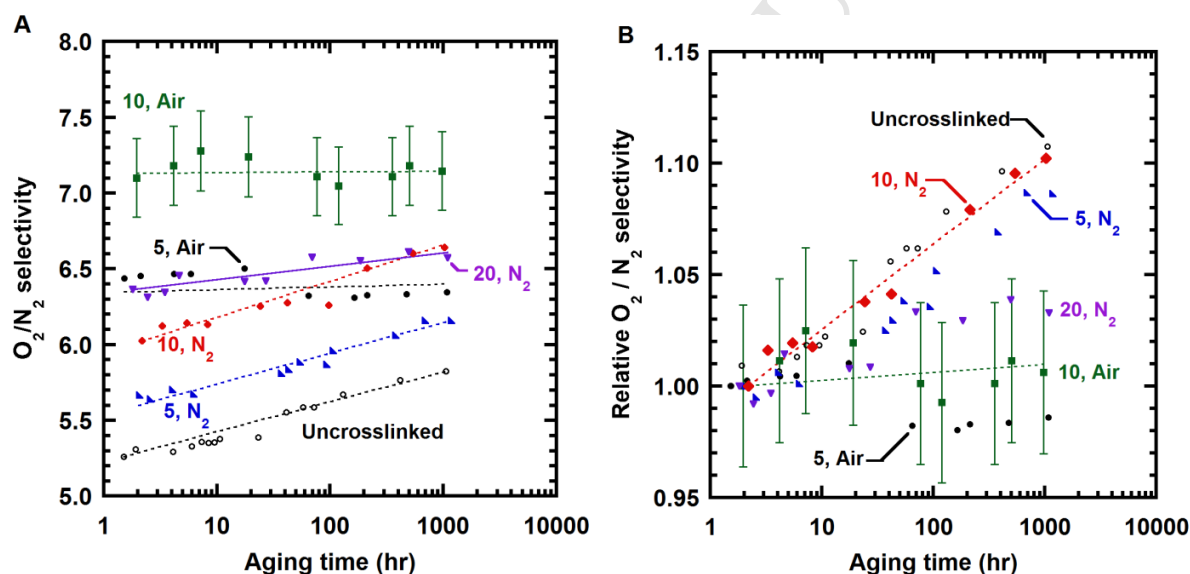

Fig. 8. Influence of physical aging on: (A) O_2/N_2 selectivity and (B) normalized O_2/N_2 selectivity of uncrosslinked and crosslinked TMBPA-BP films. In (B), data were normalized based on permeability at ~ 1 h of aging time. Samples were irradiated at 254 nm and they are designated by the total irradiation time (in min) and the irradiation environment. Lines are drawn to guide the eye.

Fig. 9 presents the influence of UV irradiation and physical aging on O_2/N_2 separation performance of TMBPA-BP thin films relative to the upper bound [59]. Transport data for thin

polysulfone (PSF) films (125 nm) are also included for comparison [14]. As polymers are UV-irradiated and undergo physical aging, the ensuing decrease in gas permeability and increase in selectivity moves transport properties in a direction parallel to but slightly away from the upper bound. Similar trends were observed in previous studies of physical aging of uncrosslinked and non-irradiated glassy polymers [3, 14, 40].
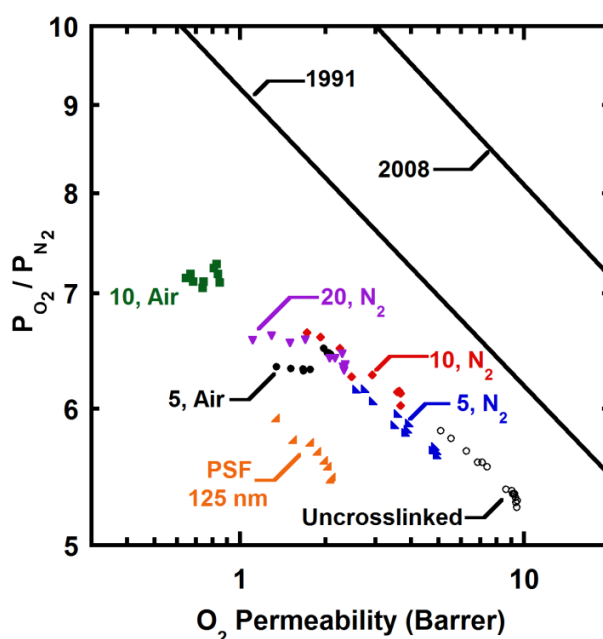

Fig. 9. Influence of physical aging and UV irradiation on O_2/N_2 separation performance of uncrosslinked and UV-irradiated TMBPA-BP samples relative to the upper bounds [59, 60]. Samples were irradiated at 254 nm. All samples were 150-170 nm thick. Transport data of ultra-thin polysulfone (125 nm thick) films are also included for reference [14]. The lines are the 1991 and 2008 upper bound limits [59, 60].

3.5 Influence of irradiation wavelength on physical aging and gas permeation properties

Fig. 10 presents the influence of UV irradiation wavelength and environment on aging behavior of TMBPA-BP thin films. Each crosslinked sample was irradiated for 10 min total (5 min/side) and is designated by the irradiation environment and wavelength. Similar to transport

properties observed for samples irradiated at 254 nm, the sample irradiated in air at 365 nm has

lower O$_2$ permeability than that irradiated in N$_2$ at 365 nm, presumably due to some

photooxidation in the sample irradiated in air, which can decrease the free volume. However, the

extent of photooxidation in the sample irradiated in air at 365 nm is probably small (relative to

that for samples irradiated at 254nm), as is evident from the similar FTIR spectra of samples

irradiated in air or N$_2$ at 365 nm (cf., Fig. 4C) and similar reductions in their benzophenone peak

intensities after irradiation (cf., Fig. 5). Consequently, films irradiated in air and N$_2$ at 365 nm

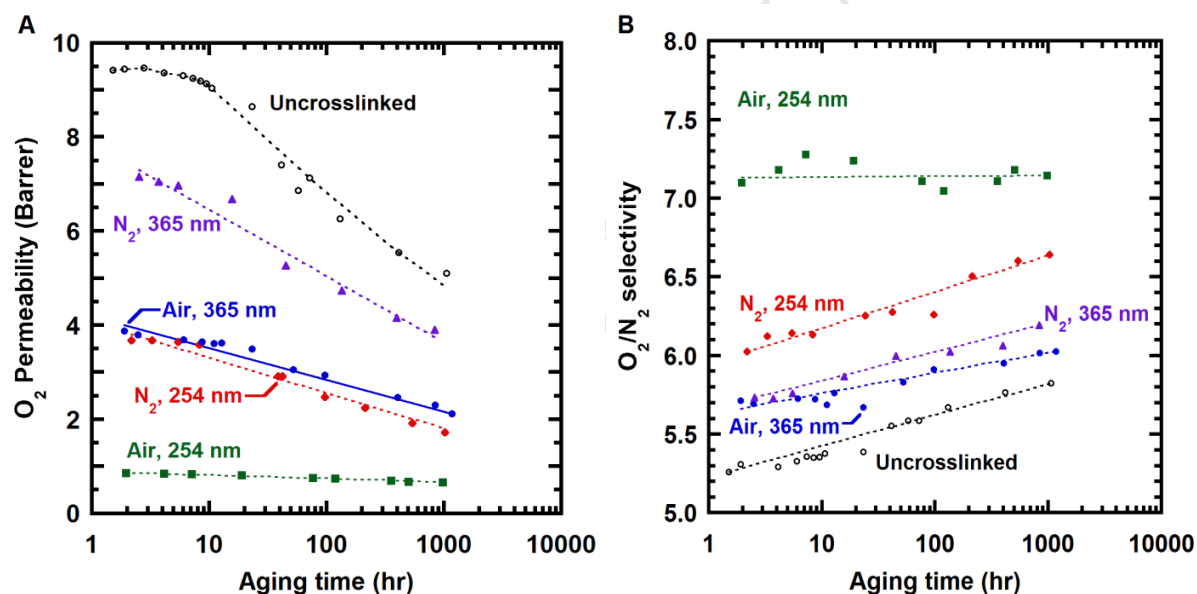have similar O$_2$/N$_2$ selectivities, as shown in Fig. 10B.

Fig. 10. Influence of crosslinking wavelength and environment on: (A) O$_2$ permeability and (B) O$_2$/N$_2$ selectivity of uncrosslinked and irradiated TMBPA-BP thin films. Each crosslinked sample was irradiated for 10 min total (5 min per side) and is designated by the irradiation environment and wavelength. All samples were 150-170 nm thick. Lines are drawn to guide the eye.

Samples irradiated at 254 nm have lower O$_2$ permeabilities and higher O$_2$/N$_2$ selectivities

than samples irradiated at 365 nm. This difference in transport properties, as well as the lower

benzophenone peak intensities for samples irradiated at 254 nm relative to those at 365 nm (cf., Fig. 5), supports the earlier hypothesis that irradiation at 254 nm may lead to more extensive crosslinking and/or photooxidation than irradiation at 365 nm.

Fig. 11 presents the influence of irradiation wavelength, irradiation environment, and physical aging on O_2/N_2 separation performance relative to the 1991 upper bound [59]. Each crosslinked sample was irradiated for 10 min (5 min per side). Transport properties of polysulfone as well as uncrosslinked and crosslinked (irradiated in N_2 at 365 nm for 7 min) tetramethyl bisphenol A benzophenone dicarboxylic acid (TMBPA-BnzDCA) are included for comparison [14, 22]. As shown in Fig. 11, at 365 nm, the properties of samples irradiated in air are somewhat farther away from the upper bound than those of the samples irradiated in N_2, because the samples irradiated in air have lower O_2 permeability coefficients yet similar O_2/N_2 selectivities as those of the samples irradiated in N_2. On the other hand, at 254 nm, the samples irradiated in air have higher selectivities and lower O_2 permeabilities than the samples irradiated in N_2, presumably due to more extensive photooxidation at 254 nm. In addition, as observed earlier, physical aging and UV irradiation move transport properties to the upper-left direction on paths that are parallel to but slightly away from the upper bound.
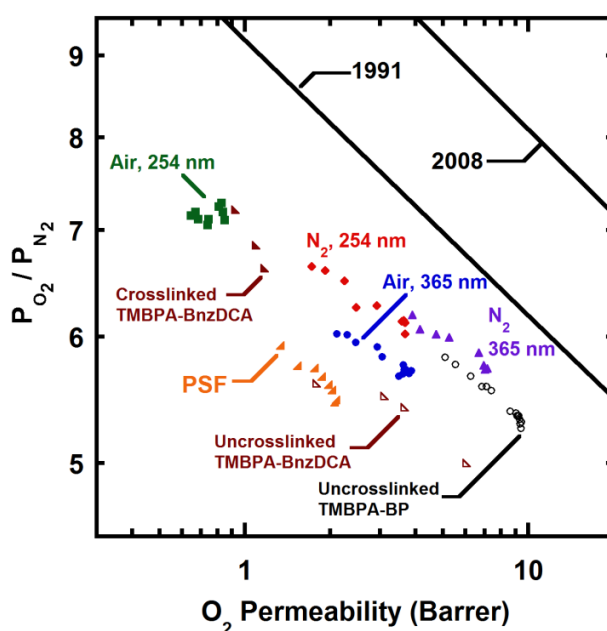
Fig. 11. Influence of irradiation wavelength, irradiation environment, and physical aging on O_2/N_2 separation performance of uncrosslinked and crosslinked TMBPA-BP samples relative to the upper bounds [59, 60]. All TMBPA-BP samples were 150-170 nm thick. Each crosslinked sample was irradiated for 10 min total (5 min per side) and is designated by the UV irradiation environment and wavelength. Physical aging of polysulfone (125 nm) [14] as well as uncrosslinked and crosslinked (irradiated in N_2 at 365 nm for 7 min) TMBPA-BnzDCA (380-860 nm thick) [22] are also included for comparison. The lines are the 1991 and 2008 upper bound limits [59, 60].

Conclusions

The influences of UV irradiation and physical aging on O_2 and N_2 transport properties of thin TMBPA-BP films were explored at 35 ^{o}C and a feed pressure of 2 atm. To investigate the influence of UV irradiation on instrinsic polymer properties, achieving a uniform dose of irradiation throughout the polymer is desired, which required using very thin films (thickness $\sim$ 150-170 nm). Both UV irradiation and physical aging decrease gas permeability coefficients and increase O_2/N_2 selectivity. Changes in transport properties became more significant as irradiation time increased, likely due to a loss in polymer free volume associated with

crosslinking and/or photooxidation. For irradiation at 254 nm, samples irradiated in air have lower permeability and higher selectivities than samples irradiated in N_2. FTIR spectra of samples irradiated in air at 254 nm showed the appearance of absorption bands ascribed to carbonyl groups, which were believed to be present in photooxidation products that were generally absent in the spectra of samples irradiated in N_2. Interactions among these polar groups can potentially decrease polymer free volume, leading to further decreases in permeability and gains in selectivity.

The influence of irradiation wavelength on transport properties was also explored. Samples were irradiated at 254 nm or 365 nm. In a fixed irradiation environment (air or N_2), samples irradiated at 254 nm were less permeable and more selective than those irradiated at 365 nm. This difference is attributed to greater UV absorption by the polymer and a higher probability of radical formation at 254 nm, both of which contribute to greater extents of crosslinking and/or photooxidation than irradiation at 365 nm. Finally, comparisons to the upper bound showed that UV irradiation and physical aging moved the transport properties mainly parallel to but slightly away from the upper bound line, a trend similar to that reported in previous aging studies on non-irradiated polymer samples.

Acknowledgments

References

1. Pfromm PH and Koros WJ. Polymer 1995;36(12):2379-2387.

2. Struik LCE. Physical aging in amorphous polymers and other materials. Amsterdam; New York: Elsevier Scientific Pub. Co., 1978.

3. Huang Y and Paul DR. Polymer 2004;45(25):8377-8393.

4. Huang Y and Paul DR. Journal of Membrane Science 2004;244(1–2):167-178.

5. Huang Y, Wang X, and Paul DR. Journal of Membrane Science 2006;277(1–2):219-229.

6. Laot CM, Marand E, Schmittmann B, and Zia RKP. Macromolecules 2003;36(23):8673-8684.

7. Hu C-C, Fu Y-J, Hsiao S-W, Lee K-R, and Lai J-Y. Journal of Membrane Science 2007;303(1–2):29-36.

8. Starannikova L, Khodzhaeva V, and Yampolskii Y. Journal of Membrane Science 2004;244(1–2):183-191.

9. Alghunaimi F, Ghanem B, Alaslai N, Swaidan R, Litwiller E, and Pinnau I. Journal of Membrane Science 2015;490:321-327.

10. Baker RW. Industrial & Engineering Chemistry Research 2002;41(6):1393-1411.

11. Sanders DF, Smith ZP, Guo R, Robeson LM, McGrath JE, Paul DR, and Freeman BD. Polymer 2013;54(18):4729-4761.

12. Cui L, Qiu W, Paul DR, and Koros WJ. Polymer 2011;52(15):3374-3380.

13. McCaig MS and Paul DR. Polymer 2000;41(2):629-637.

14. Rowe BW, Freeman BD, and Paul DR. Polymer 2009;50(23):5565-5575.

15. Kita H, Inada T, Tanaka K, and Okamoto K-i. Journal of Membrane Science 1994;87(1–2):139-147.

16. Tillet G, Boutevin B, and Ameduri B. Progress in Polymer Science 2011;36(2):191-217.

17. Wind JD, Staudt-Bickel C, Paul DR, and Koros WJ. Macromolecules 2003;36(6):1882-1888.

18. Lin AA, Sastri VR, Tesoro G, Reiser A, and Eachus R. Macromolecules 1988;21(4):1165-1169.

19. Vanherck K, Koeckelberghs G, and Vankelecom IFJ. Progress in Polymer Science 2013;38(6):874-896.

20. Wright CT and Paul DR. Journal of Membrane Science 1997;124(2):161-174.

21. Dudley CN, Schöberl B, Sturgill GK, Beckham HW, and Rezac ME. Journal of Membrane Science 2001;191(1–2):1-11.

22. McCaig MS and Paul DR. Polymer 1999;40(26):7209-7225.

23. Meier IK and Langsam M. Journal of Polymer Science Part A: Polymer Chemistry 1993;31(1):83-89.

24. Meier IK, Langsam M, and Klotz HC. Journal of Membrane Science 1994;94(1):195-212.

25. Matsui S, Ishiguro T, Higuchi A, and Nakagawa T. Journal of Polymer Science Part B: Polymer Physics 1997;35(14):2259-2269.

26. Matsui S, Sato H, and Nakagawa T. Journal of Membrane Science 1998;141(1):31-43.

27. Matsui S and Nakagawa T. Journal of Applied Polymer Science 1998;67(1):49-60.

28. Liu Q, Characterization of gas separation properties of novel polymer membranes (Doctoral dissertation, University of Texas at Austin, Austin, TX, USA). 2015.

29. Chng ML, Xiao Y, Chung TS, Toriida M, and Tamai S. Polymer 2007;48(1):311-317.

30. Wu SK and Rabek JF. Polymer Degradation and Stability 1988;21(4):365-376.

31. Scaiano JC, Netto-Ferreira JC, Becknell AF, and Small RD. Polymer Engineering & Science 1989;29(14):942-944.

32. Sundell BJ, Shaver AT, Liu Q, Nebipasagil A, Pisipati P, Mecham SJ, Riffle JS, Freeman BD, and McGrath JE. Polymer 2014;55(22):5623-5634.

33. Zigeuner G, Fuchs E, Brunetti H, and Sterk H. Monatshefte für Chemie und verwandte Teile anderer Wissenschaften 1966;97(1):36-42.

34. Tiwari RR, Smith ZP, Lin H, Freeman BD, and Paul DR. Polymer 2014;55(22):5788-5800.

35. Horn NR and Paul DR. Polymer 2011;52(7):1619-1627.

36. Henis JMS and Tripodi MK. Separation Science and Technology 1980;15(4):1059-1068.

37. Henis JMS and Tripodi MK. Multicomponent membranes for gas separations. Patent No. 4230463. United States: Monsanto Company (St. Louis, MO), 1980.

38. Henis JMS and Tripodi MK. Journal of Membrane Science 1981;8(3):233-246.

39. Henis JMS and Tripodi MK. Science 1983;220(4592):11-17.

40. Murphy TM, Freeman BD, and Paul DR. Polymer 2013;54(2):873-880.

41. Lin H and Freeman BD. Springer Handbook of Materials Measurement Methods 2006:371-387.

42. Paul DR. Journal of Membrane Science 1984;18:75-86.

43. Shin-Etsu Chemical, Characteristic properties of silicone rubber compounds [Online]; 2012; http://www.shinetsusilicone-global.com/catalog/pdf/rubber_e.pdf (accessed October 22, 2015).

44. Graubner V-M, Jordan R, Nuyken O, Schnyder B, Lippert T, Kötz R, and Wokaun A. Macromolecules 2004;37(16):5936-5943.

45. Schnyder B, Lippert T, Kötz R, Wokaun A, Graubner V-M, and Nuyken O. Surface Science 2003;532–535:1067-1071.

46. Efimenko K, Wallace WE, and Genzer J. Journal of Colloid and Interface Science 2002;254(2):306-315.

47. Balzani V, Ceroni P, and Juris A. Photochemistry and Photophysics: Concepts, Research, Applications: Wiley, 2014.

48. Kuroda S-i and Mita I. European Polymer Journal 1989;25(6):611-620.

49. Silverstein RM, Webster FX, and Kiemle D. Spectrometric identification of organic compounds, Seventh ed.: Wiley Global Education, 2005.

50. Turro NJ, Dalton JC, Dawes K, Farrington G, Hautala R, Morton D, Niemczyk M, and Schore N. Accounts of Chemical Research 1972;5(3):92-101.

51. Reusch W. Photochemistry. In *Virtual Textbook of Organic Chemistry* [Online]; 1999; https://www2.chemistry.msu.edu/faculty/reusch/VirtTxtJml/photchem.htm (accessed October 21, 2015).

52. Atkins P and de Paula J. Physical Chemistry: W. H. Freeman, 2006.

53. Kim JH, Koros WJ, and Paul DR. Journal of Membrane Science 2006;282(1–2):32-43.

54. Sanders DF, Guo R, Smith ZP, Stevens KA, Liu Q, McGrath JE, Paul DR, and Freeman BD. Journal of Membrane Science 2014;463:73-81.

55. Rowe BW, Freeman BD, and Paul DR. Macromolecules 2007;40(8):2806-2813.

56. Horn NR and Paul DR. Polymer 2011;52(24):5587-5594.

57. Poling B, Prausnitz J, and Connell JO. The properties of gases and liquids, Fifth ed.: McGraw-Hill Education, 2000.

58. Bevington PR and Robinson DK. Data reduction and error analysis for the physical sciences, Third ed.: McGraw-Hill, 2003.

59. Robeson LM. Journal of Membrane Science 1991;62(2):165-185.

60. Robeson LM. Journal of Membrane Science 2008;320(1–2):390-400.

Highlights

- Submicron poly(arelene ether ketone) copolymer films were UV irradiated.
- Permeability increases and selectivity decreases with increasing UV irradiation time and aging time.
- Gas permeation properties depend on UV irradiation environment.
- Aging environment influences polymer aging behavior.